

Pharmaceutical Nanotechnology

# Nanoscopic friction behavior of pharmaceutical materials

Jonghwi Lee\*

*Department of Chemical Engineering and Materials Science, Chung-Ang University,  
221 Heukseok-dong, Dongjak-gu, Seoul 156-756, South Korea*

Received 14 January 2007; accepted 15 March 2007

Available online 19 March 2007

## Abstract

The characteristics of various pharmaceutical dosage forms are influenced by surface properties such as the friction behavior. For example, die wall friction is a key issue in developing a solid dosage form. However, the friction properties are not completely understood mainly because of the lack of fundamental measurements. Herein, the friction behavior of pharmaceutical materials was investigated and compared with their adhesion behavior using atomic force microscopy. The sliding speed causes significant variations in the frictional force. Compared with other materials, lubricant materials showed less distinct differences in friction tests than in adhesion tests, indicating the dependence of the lubricant efficiency on the stress state. The three parameters obtained from the modified Amonton's law, i.e., absolute frictional force, friction coefficient and residual force, showed consistent trends. Overall, the friction behavior was not a direct reflection of the adhesion forces. The intrinsic friction behavior of a single pharmaceutical particle can be quantified using atomic force microscopy.

© 2007 Elsevier B.V. All rights reserved.

*Keywords:* Atomic force microscopy (AFM); Adhesion; Flowability; Acetaminophen

## 1. Introduction

Pharmaceutical dosage forms contain more than one component, and the construction of a delivery system out of the components depends on their surface properties (Lee, 2004, 2005; Simons et al., 2003; Michrafy et al., 2004; Podczeczek et al., 1995; Lam and Newton, 1991; Podczeczek, 1998a,b, 1999; Ibrahim et al., 2000). Surface interactions between two particles or a particle and the processing equipment influence the parameters of a pharmaceutical formulation such as density distribution, tablet strength, blending uniformity, flow characteristics, granulation, disintegration, etc. (Lee, 2004, 2005; Podczeczek et al., 1995; Lam and Newton, 1991; Alderborn and Nystrom, 1996; Hayama et al., 2003; Berard et al., 2002; Louey et al., 2001; Carstensen, 2001). Surface interactions are not simply based on van der Waals interactions. There are many other factors that need to be considered carefully such as electrostatic, capillary, specific chemical bonding interactions, etc. (Lee, 2004, 2005; Israelachvili, 2002). This also depends on the applied stress conditions because the material response is a function of the

stress conditions. The adhesion force mainly concerns the normal stress conditions, and the frictional force related to the shear conditions.

Friction is a measure of the interaction between surfaces in relative motion (Israelachvili, 2002). Generally, a solid with a higher surface energy has a higher level of friction than that with a lower surface energy (Israelachvili, 2002). The adhesion force is not always related to the frictional force (Yoshizawa and Israelachvili, 1994; Yoshizawa et al., 1993). There are many cases with a strong adhesive force with a relatively low frictional force and vice versa. It was reported in some cases that adhesion hysteresis is more important for assessing the friction force than the surface energy (Chaudhury and Owen, 1993).

The friction behavior has been an important subject for decades, but there is a little fundamental understanding and measurement technique of this behavior in the pharmaceutical area (Michrafy et al., 2004; Podczeczek et al., 1995; Alderborn and Nystrom, 1996; Bhushan and Kionkar, 1994). For example, solid dosage forms are being made using a metal die, and die sticking continues to be a serious problem in the pharmaceutical unit operation (Lee, 2004; Alderborn and Nystrom, 1996). Most pharmaceutical industries use empirical approaches to deal with these problems. Despite the importance of the problems

\* Tel.: +82 2 8205269; fax: +82 2 8243495.

E-mail address: [jong@cau.ac.kr](mailto:jong@cau.ac.kr).

associated with the sticking behavior, the problem solving strategy is suffering a lack of fundamental understanding.

The macroscopic friction behavior and related pharmaceutical problems reflect the properties of individual or multiple particle(s), i.e., particle size, shape, density, size distribution, etc. The properties of particles are based on their nanoscopic properties, i.e., intrinsic friction per unit surface area of a single particle (Simons et al., 2003; Louey et al., 2001; Sindel and Zimmermann, 2001). Indeed, measuring the friction on the nanometer scale is intriguing because it can be a starting point for a systematic analysis of macroscopic friction (Bhushan and Kionkar, 1994; Clear and Nealey, 1999; Bergström and Meurk, 2002; Tsukruk and Bliznyuk, 1998; Kim et al., 2002; Noy et al., 1995; Frisbie et al., 1994). A direct relationship between the nanoscopic observations and the macroscopic problems of many particle systems is a separate subject because of the many other intervening parameters.

Atomic force microscopy (AFM) has been used to examine the nanoscopic properties of various materials (Yoshizawa and Israelachvili, 1994; Yoshizawa et al., 1993; Chaudhury and Owen, 1993; Bhushan and Kionkar, 1994; Clear and Nealey, 1999; Bergström and Meurk, 2002; Tsukruk and Bliznyuk, 1998; Kim et al., 2002; Ducker et al., 1991, 1992; Haugstad and Gladfelter, 1994; Tortonese and Kirk, 1997). A particle can be attached onto a cantilever, and the interactions when it comes into contact with another particle surface can be measured by AFM. The surface frictional forces cause the cantilever to twist when it is moved back and forth perpendicular to the cantilever axis (Ducker et al., 1991). AFM measures the degree of twisting, normal deflection, and the *z*-position of the cantilever, which are later converted to frictional and normal force data. The first observations of the friction and stick–slip behavior on the nanometer scale using AFM were reported in 1990. Shortly after, the successful measurements of adhesion (normal force) between two surfaces were reported (Ducker et al., 1991, 1992; Mate et al., 1987).

Our previous reports (Lee, 2004, 2005) focused on the adhesion behavior of pharmaceutical materials under a normal stress state. In particular, the sticking problems in compaction were our target (Lee, 2004). Thus, a stainless steel particle was attached to a tipless cantilever and used as the AFM probe against the surfaces of various pharmaceutical materials ranging from lubricants to drug particles. Distinct differences between the adhesion properties of various particles were found. The adhesion forces of lubricants were generally less than one-third of those of other pharmaceutical materials (Lee, 2004).

The sticking issues are related not only with surface adhesion but also with friction between the particles and die wall. Significant particle movement during compaction makes the frictional force a key concern (Aldern and Nystrom, 1996). Therefore, this study made a systematic assessment of the friction behavior of pharmaceutical materials. For comparison, the same pharmaceutical materials and AFM used in our previous investigation on adhesion forces (Lee, 2004) were used in this study. In this approach, the mode of AFM operation and the size of the interacting surface area were different. The friction coefficients were

assessed by varying the normal force and compared with the adhesion forces previously reported (Lee, 2004). To the best of our knowledge, the friction behavior of common pharmaceutical materials has never been examined. This study highlights the feasibility and applicability of AFM friction techniques for pharmaceutical research and development.

## 2. Materials and methods

### 2.1. Materials

Stainless steel spherical particles were obtained from AISI 316 powder (Goodfellow). Magnesium stearate (MS, Mallinkrodt), sodium stearyl fumarate (SF, Pruv<sup>®</sup>, Pen-West), lactose monohydrate fast flo (LT, Foremost), and acetaminophen (AP, Aldrich, *N*-acetyl-*p*-aminophenol) were used as received. Norland optical adhesive 81 was used to immobilize the particles, which was a typical one for minimizing possible surface contamination from its own evaporable components. Further details are reported elsewhere (Lee, 2004, 2005).

### 2.2. Sample preparation

The immobilized particle beds or compacts were used for the friction tests. Compacts of LT and AP were prepared under 100 MPa for a 10 s dwell time using a Carver press hydraulic unit #3912. In order to have a flat surface for the AFM examination, one face of the compact was covered with a silicon wafer that had previously been cleaned with *n*-heptane and ethanol for 2 min. Although the silicon wafer often broke during compaction, a flat surface sufficiently large for AFM investigations was obtained. The MS and SF particles were attached to glass slides with a thin layer of the same adhesive. The estimated thickness of the layer was <1 μm based on optical microscopy observations of the thickness and interference color (Hecht, 1987). The particles were immobilized by curing the adhesive using a spectroline UV lamp (Model UV-4B, 365 nm) for 30 min (10 cm away from the light source).

### 2.3. Characterizations of particles

For an AFM topographical investigation, a Dimension<sup>™</sup> 3100 scanning probe microscope (Digital Instruments) with a DI DAFMF2X closed loop scanner head was used on a VT-103-3K Isolation System table. An 1 μm × 1 μm surface was scanned in tapping mode under ambient conditions using TESP or TESP7 etched single crystal silicon probes (Digital Instruments, 20–100 N/m force constant and 200–400 kHz resonance frequency). The surface roughness was calculated from 10 surface images using SPIP software (Image Metrology Aps., version 2.3214).

### 2.4. AFM measurements

The stainless steel tips were prepared using micro- and nano-manipulators, a KITE-R (World Precision Instruments) and

a specimen stage of a microindenter (CSEM Micro-hardness tester). The AFM cantilever used was a Nanoprobe™ SPM DNP-S. A sphere was attached onto the tip region of a cantilever using a limited amount of adhesive, which was later cured using a UV lamp for 30 min. The friction measurements were performed at a scan size of 2 μm × 2 μm. The samples were scanned back and forth in a direction orthogonal to the longitudinal direction of the cantilever beam. The amount of cantilever twisting was recorded, and the resulting friction loop (Fig. 1a) was analyzed. The particle tips prepared as described above were used. Therefore, simultaneous measurements of the frictional force and surface roughness, which is commonly used for eliminating the effect of misalignment, were not possible (Mate et al., 1987). During the measurements, the temperature was set to 19.6–20.7 °C. The lateral (shear) spring constant,  $k_{lat}$ , was calculated from the measured normal spring constant,  $k$ , using the

method reported in the literature (Noy et al., 1995). Briefly,  $k_{lat}$  is

$$k_{lat} = \frac{2}{6 \cos^2 \theta + 3(1 + \gamma) \sin^2 \theta} \left(\frac{L}{H}\right)^2 k$$

where  $\theta$  is the angle between the base arms of the triangular cantilever,  $\gamma$  the Poisson ratio,  $L$  the length of the cantilever beam and  $H$  is the length of tip. The normal  $k$  was measured using the method described elsewhere (Tortonese and Kirk, 1997). (Typical values:  $k=0.1149$ ,  $k_{lat}=1.2414$ .) The method based on the beam theories provides only limited accuracy but was sufficient for this comparison study (Tortonese and Kirk, 1997; Sader et al., 1995; Cleveland et al., 1993). Unless otherwise specified, the scanning speed was 2.00 μm/s. The statistical distribution of the frictional force data was checked each time following the method reported elsewhere (Sindel and Zimmermann, 2001; Tortonese

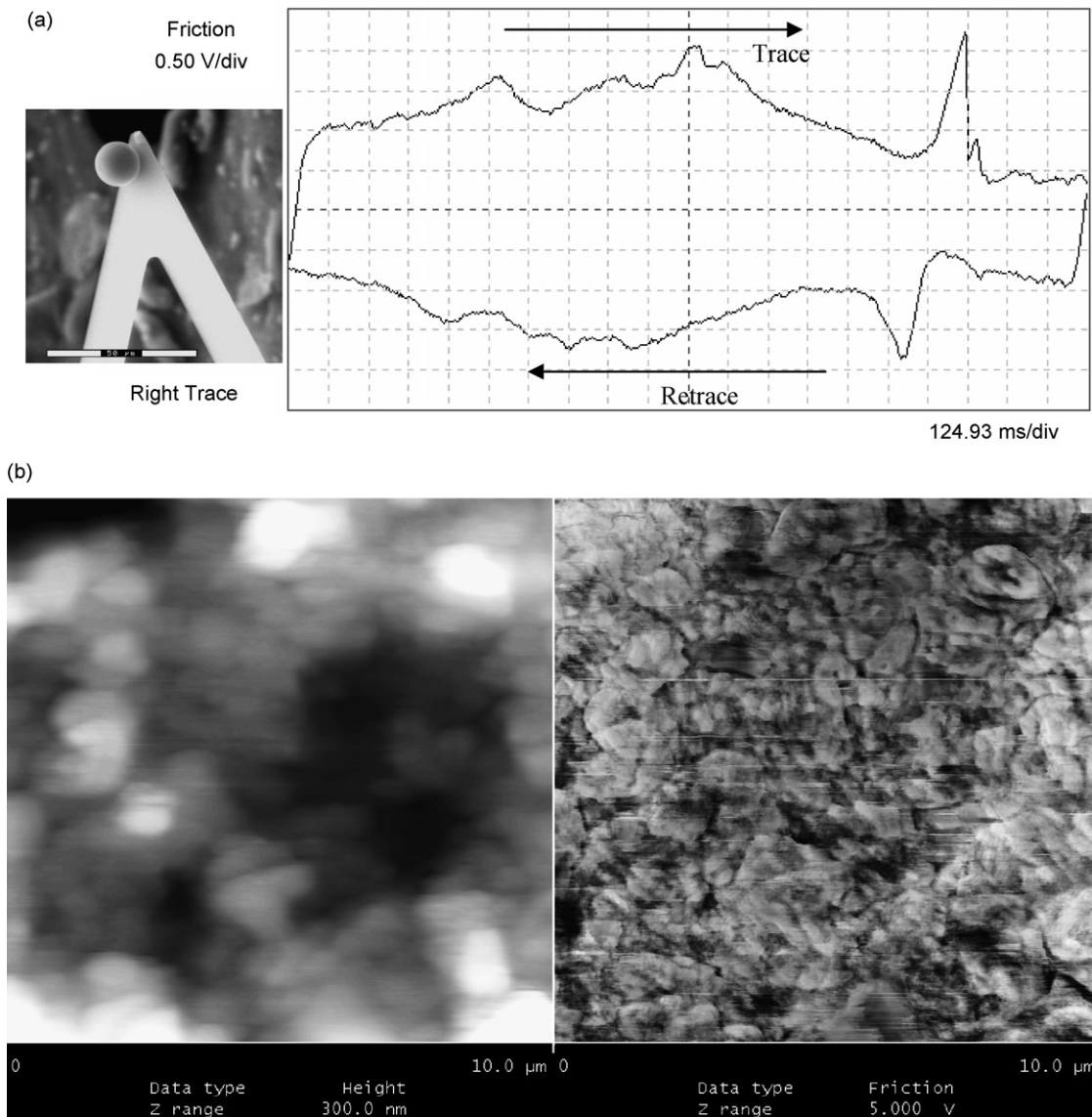


Fig. 1. Typical raw data (friction loop) of AFM friction measurements and ESEM micrograph of AFM cantilever modified by a stainless steel sphere (a) and AFM height (left) and friction (right) images of the surface of a LT compact (b). The scale bar inside the ESEM micrograph is 50 μm. In the friction loop of LT, the y- and x-axis are the detector signal and the lateral displacement of the sample perpendicular to the principal axis of a cantilever for 2 μm trace–retrace cycles, respectively.

and Kirk, 1997; Beach et al., 2002; Fuji et al., 1999; Xiao and Qian, 2000; Li et al., 1993; Larson et al., 1993; Villarrubia, 1994; Eve et al., 2002). The possibility of surface contamination was checked using the procedure reported in the literature (Lee, 2004).

### 3. Results

In order to understand the friction behavior of pharmaceutical materials, some essential properties need to be mentioned as background information. The other general physical properties are available elsewhere (Lee, 2004). The radius of the stainless steel particle attached to the cantilever was  $15.05 (\pm 0.02) \mu\text{m}$ . The root-mean-square (r.m.s.) surface roughness values of the stainless steel, MS, SF, LT and AP measured by AFM were  $4.2 (\pm 2.7)$ ,  $44.6 (\pm 12.1)$ ,  $23.4 (\pm 2.3)$ ,  $21.5 (\pm 6.0)$ , and  $4.0 (\pm 3.3) \text{nm}$ , respectively. These values can affect the absolute frictional and normal forces but theoretically do not affect the friction coefficients. Many macroscopic measurements have shown that there is no correlation between both the average and r.m.s. surface roughness values and the relative values of the adhesion forces of pharmaceutical materials (Podczeczek et al., 1995; Podczeczek, 1998a,b, 1999).

The frictional force measurements provide loop type raw data (friction loop) showing cantilever twisting depending on the scanning direction. Fig. 1a shows a typical friction loop where a trace and a retrace curve form a closed loop, and one-half of the difference between them corresponds to the frictional force. The lateral spring constant of the cantilever and the sensitivity of the optical detector were used to convert the raw data, as described above. In Fig. 1a, no significant stick–slip behavior was observed, as reported elsewhere (Israelachvili, 2002). The details of the friction loop often reflect the surface topology, even though the effect of the surface topology on the friction coefficient can be negligible. In addition, Fig. 1a shows the misfit between the peaks of the trace and retrace curves.

A friction loop curve does not necessarily reflect the surface topology. This is supported by Fig. 1b, which shows the differences between the height and friction images. Features clearly visible in the height image are not always noticeable in the other image. Therefore, the result obtained from the frictional force measurement can be treated as separate information distinct from the one obtained from the height (or even phase) imaging.

There are many variables that are important when measuring the frictional force. Among them, the effect of the sliding speed of a cantilever on the frictional force was found to be significant (Fig. 2). The frictional force rapidly increases as the sliding speed increases up to  $2 \mu\text{m/s}$ . Within the operating window of the AFM, the frictional forces appear to reach their steady-state values at a sliding speed  $>2 \mu\text{m/s}$  regardless of the normal force. A slight decrease in the frictional forces might be noticed  $>2 \mu\text{m/s}$ , but these changes are within the experimental error.

Fig. 3 shows the typical relationship between the normal and frictional forces. The data points were obtained during the step increase (loading) and subsequent decrease (unloading) in the normal force by controlling the set point of the AFM. In all data

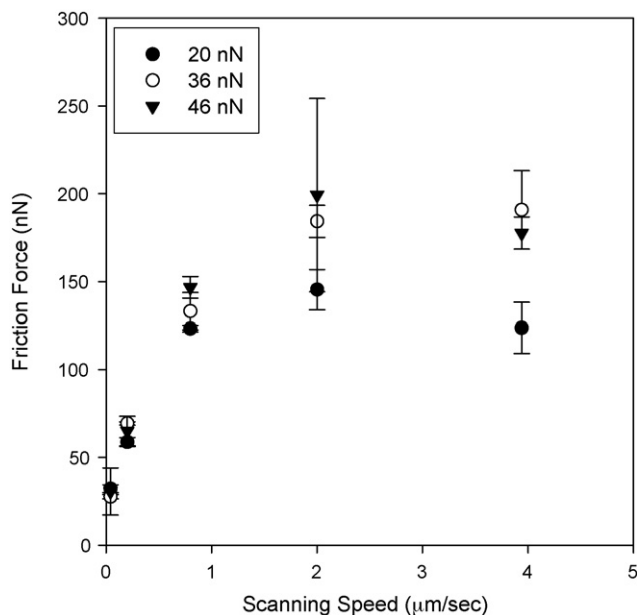


Fig. 2. Effect of sliding speed on the friction force between stainless steel and AP under various normal forces (20, 36, and 46 nN).

sets, the slope of unloading (open symbols) is always smaller than that of loading (closed symbols), and the unloading data has higher absolute force values than the loading data. The significant hysteresis between the loading and unloading results arises mainly from the hysteresis in the frictional force, not from the hysteresis in the normal force. The possible hysteresis in the normal force was checked without lateral movement. The plot of the normal force as a function of the set point in Fig. 4 shows that any hysteresis is insignificant. The changes in the set point trigger little variation in the normal forces. Most of the data points of loading precisely overlap those of unloading.

The absolute values of the frictional force were directly related to the residual forces in the modified Amonton's law

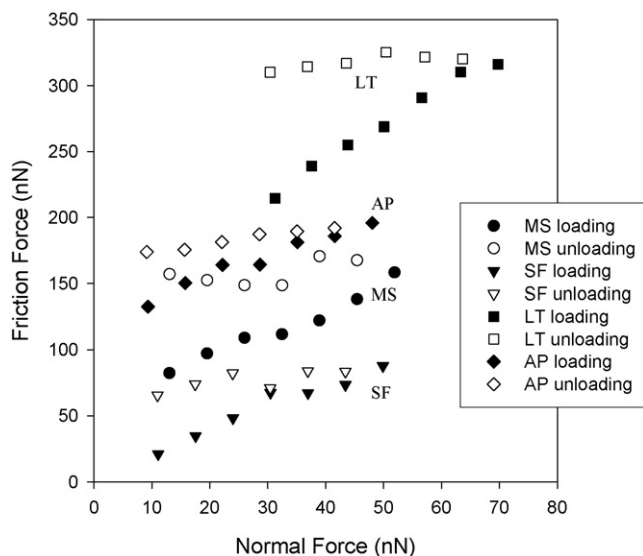


Fig. 3. Friction force development as a function of normal force in stainless steel/AP during loading (closed symbols) and unloading (open symbols).

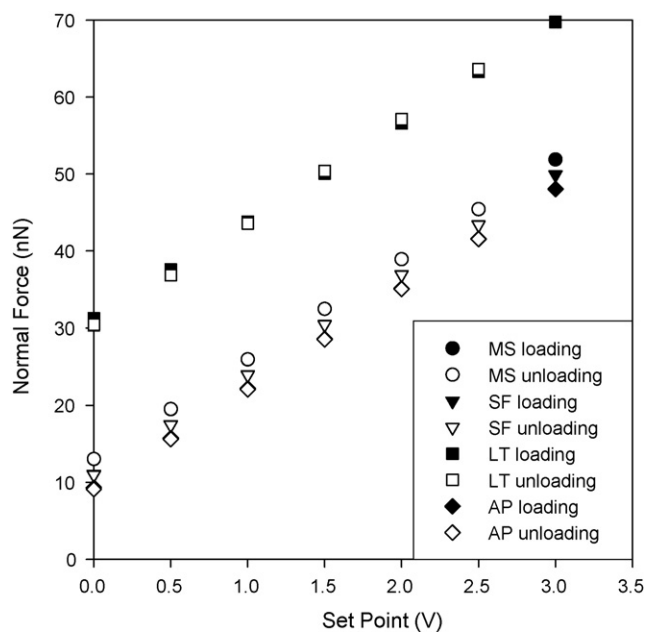


Fig. 4. Normal force development as a function of set point in stainless steel/AP during loading and unloading.

(Yoshizawa et al., 1993; Bergström and Meurk, 2002; Heim et al., 1999). The residual forces were higher in the following order: LT (303 nN, correlation coefficient,  $cc = 0.050$ ), AP (181 nN,  $cc = 0.021$ ), MS (92 nN,  $cc = 0.070$ ), and SF (42 nN,  $cc = 0.137$ ) (average values from 65 repeated measurements). Each one of them showed rather different residual force values, while all the friction coefficients were in the same order (Fig. 5).

The reason why the absolute force of LT was significantly higher than the others (Fig. 3) might be due to differences in the contact area. The contact area between the stainless steel particle tip and the pharmaceutical particles was neither controlled nor measured. Therefore, the absolute values of the frictional force and residual force would vary significantly because each engagement of a stainless steel particle tip results in a different contact area. Fig. 3 shows the typical data for each material.

To calculate the friction coefficients, the results of 65 measurements were averaged. Fig. 5 shows the average values with the adhesion force data previously reported (Lee, 2004). The friction coefficients of the two lubricants, i.e., MS and SF, were generally lower than those of LT and AP, which is a similar trend to what the adhesion force result shows. However, the difference in the friction coefficient between the lubricants (MS and SF) and the others was much smaller than the difference in the adhesion force. While the adhesion forces of MS and SF are <25% of the adhesion force of AP, the frictional forces of MS and LT are only marginally smaller than that of AP. Hence, the role of pharmaceutical lubricants appears to originate from their adhesion properties and not from their friction properties. Furthermore, AP has a much higher adhesion force but a slightly smaller friction coefficient than LT. These results are consistent with the knowledge that the friction coefficient does not reflect the absolute values of the adhesion force (Yoshizawa and Israelachvili, 1994; Yoshizawa et al., 1993).

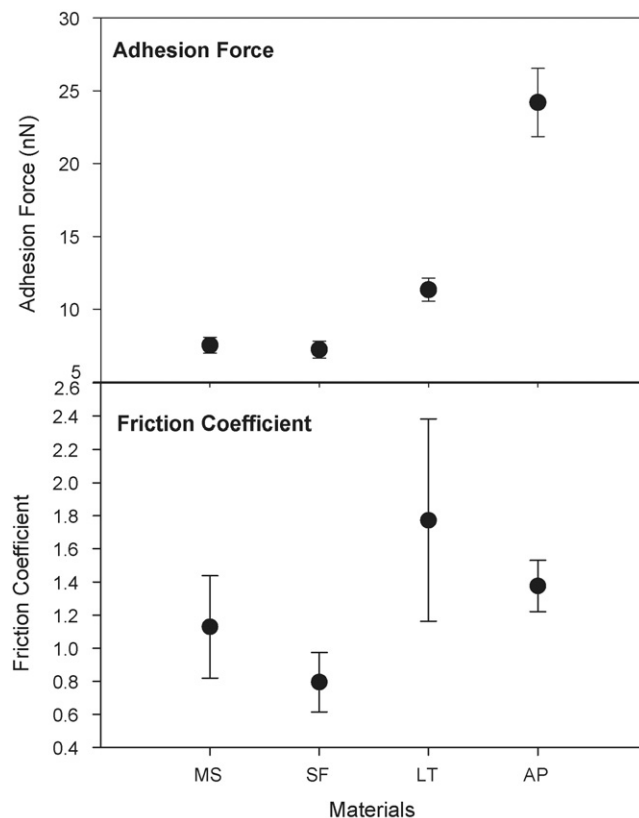


Fig. 5. Comparison between friction coefficients and adhesion forces of various pharmaceutical materials with stainless steel. The adhesion force data are taken from the previous report (Lee, 2004) for comparison.

#### 4. Discussion

The fundamentals of the friction coefficient were successfully described by Amontons' law, which defines the coefficient,  $\mu$ , as  $F_f/W$ , where  $F_f$  denotes the frictional force and  $W$  is the force normal to the surface (Israelachvili, 2002; Yoshizawa et al., 1993; Bergström and Meurk, 2002; Heim et al., 1999). According to the original hypothesis, the coefficient is independent of the contact area and normal force. The common friction results in a better fit to the linear function of the applied normal force with a nonzero intercept, which is a more generalized treatment (modified Amontons' law) (Yoshizawa et al., 1993; Bergström and Meurk, 2002; Heim et al., 1999). The frictional force is related to the applied normal force as follows:

$$F_f = \mu W + F_o$$

where  $\mu$  is the kinetic friction coefficient and  $F_o$  is the residual force or force that is not accounted for by the spring normal force. The residual force is considered to be a function of the surface free energy.

More complicated aspects need to be considered for the actual frictional force measurements. Friction generates surface deformation and a local increase in temperature. In most actual friction cases, the initial contact between two surfaces causes deformation eventually leading to multiple contacts. Therefore, the true contact area, which is much less than the initial (apparent) area, is hard to quantify. It significantly depends on the

normal force and loading history. When the normal force is relatively large, the contact area is determined by the yield pressure of the material, and when normal force is small, the contact area often scales with two-thirds of the normal force (Yoshizawa and Israelachvili, 1994; Yoshizawa et al., 1993; Bhushan and Sundararajan, 1998). Local increases in temperature due to friction can cause surface deformation, changes in the contact area, modification of the surface materials, properties, etc. These kinetic influences can be added to intrinsic friction properties, and might be a major factor in determining the scanning speed dependence of the frictional force shown in Fig. 2. Therefore, a slight change in frictional force, even above 2  $\mu\text{m/s}$ , is not surprising.

Similar to what the previous adhesion results have shown (Lee, 2004), the characteristics of two common pharmaceutical lubricants, MS and SF, were confirmed again in the three friction results, i.e., absolute frictional force, friction coefficient and residual force. These materials have unique adhesion and friction behavior that is different from other pharmaceutical particles. However, compared with the adhesion results (Lee, 2004), their relative differences in friction were rather small, often within the error (Fig. 5). The intrinsic friction properties of MS and SF might contribute less to their lubrication capabilities than to their intrinsic adhesion properties. This means that the lubrication effect would be better under normal stress than under shear stress conditions. It is natural that materials respond differently under different stress conditions.

According to the previous discussion, reducing friction appears to be less effective than reducing the level of adhesion using the same amount of MS or SF. However, this can only be true if other macro- and microscopic characteristics such as the particle size, shape, aspect ratio, etc. can be kept constant. The macroscopic friction behavior could be noticeably different from the nanoscopic behavior. Nevertheless, the single particle friction results obtained in this study are important intrinsic factors in determining the macroscopic behavior. Although further studies will be needed to interconnect the nanoscopic behavior with the macroscopic one, single particle friction measurement is a useful starting point for understanding the complicated behavior of pharmaceutical materials.

## 5. Conclusions

The intrinsic friction behavior of single pharmaceutical particles was successfully examined using atomic force microscopy. A stainless steel sphere was used as the probe attached onto a cantilever, and its interactions with particles of magnesium stearate, sodium stearyl fumarate, lactose, and acetaminophen were examined. The typical friction loop curves did not show stick–slip friction, which is common in macroscopic friction tests. The sliding speed effect was found to be significant suggesting the existence of kinetic influences. Compared with the previous study on the adhesion behavior of the same materials, the friction measurements showed relatively small differences in the friction coefficients of the different materials. The relative order between the friction coefficients of lactose and acetaminophen was different from that between their adhe-

sion forces. This is consistent with the comparison between the friction and height images. These results show that there is no significant correlation between the friction coefficient and the adhesion force. The decrease in friction using magnesium stearate or sodium stearyl fumarate might be less efficient than the decrease in adhesion using the same materials.

## Acknowledgements

This work was supported by Korean Energy Management Corporation R&D project number 2006-E-ID11-P-30-3-020. JL appreciates E. Dokou, G. Shi, and X.-Y. Fu at Merck & Co. for their technical suggestion on AFM.

## References

- Alderborn, G., Nystrom, C., (Eds.), 1996. *Pharmaceutical Powder Compaction Technology*, Marcel Dekker.
- Beach, E.R., Tormoen, G.W., Drelich, J., Han, R., 2002. Pull-off measurements between rough surfaces by atomic force microscopy. *J. Colloid Interf. Sci.* 247, 84–99.
- Berard, V., Lesniewska, E., Andres, C., Pertuy, D., Laroche, C., Pourcelot, Y., 2002. Dry powder inhaler: influence of humidity on topology and adhesion studied by AFM. *Int. J. Pharm.* 232, 213–224.
- Bergström, L., Meurk, A., 2002. Measuring granule friction and adhesion with an atomic force microscope. *Key Eng. Mater.* 63, 206–213.
- Bhushan, B., Kionkar, V.N., 1994. Tribological studies of silicon for magnetic recording applications. *J. Appl. Phys.* 75, 5741–5746.
- Bhushan, B., Sundararajan, S., 1998. Micro/nanoscale friction and wear mechanisms of thin films using atomic force and friction force microscopy. *Acta Mater.* 46, 3793–3804.
- Carstensen, J.T., 2001. *Advanced Pharmaceutical Solids*. Marcel Dekker.
- Chaudhury, M.K., Owen, M.J., 1993. Adhesion hysteresis and friction. *Langmuir* 9, 29–31.
- Clear, S.C., Nealey, P.F., 1999. Chemical force microscopy study of adhesion and friction between surfaces functionalized with self-assembled monolayers and immersed in solvents. *J. Colloid Interf. Sci.* 213, 238–250.
- Cleveland, J.P., Manne, S., Bocek, D., Hansma, P.K., 1993. A nondestructive method for determining the spring constant of cantilevers for scanning force microscopy. *Rev. Sci. Instrum.* 64, 403–405.
- Ducker, W.A., Senden, T.J., Pashley, R.M., 1991. Direct measurement of colloidal forces using an atomic force microscope. *Nature* 353, 239–241.
- Ducker, W.A., Senden, T.J., Pashley, R.M., 1992. Measurement of forces in liquids using a force microscope. *Langmuir* 8, 1831–1836.
- Eve, J.K., Patel, N., Luk, S.Y., Ebbens, S.J., Roberts, C.J., 2002. A study of single drug particle adhesion interactions using atomic force microscopy. *Int. J. Pharm.* 238, 17–27.
- Frisbie, C.D., Rozsnyai, L.F., Noy, A., Wrighton, M.S., Lieber, C.M., 1994. Functional group imaging by chemical force microscopy. *Science* 265, 2071–2074.
- Fuji, M., Machida, K., Takei, T., Watanabe, T., Chikazawa, M., 1999. Effect of wettability on adhesion force between silica particles evaluated by atomic force microscopy measurement as a function of relative humidity. *Langmuir* 15, 4584–4589.
- Haugstad, G., Gladfelter, W.L., 1994. Probing biopolymers with scanning force methods: adsorption, structure, properties, and transformation of gelatin on mica. *Langmuir* 10, 4295–4306.
- Hayama, M., Yamamoto, K., Kohori, F., Uesaka, T., Ueno, Y., Sugaya, H., Itagaki, I., Sakai, K., 2003. Nanoscopic behavior of polyvinylpyrrolidone particles on polysulfone/polyvinylpyrrolidone film. *Biomaterials* 25, 1019–1028.
- Hecht, E., 1987. *Optics*. Addison-Wesley, p. 334.
- Heim, L.-O., Blum, J., Preuss, M., Butt, H.-J., 1999. Adhesion and friction forces between spherical micrometer-sized particles. *Phys. Rev. Lett.* 83, 3328.

- Ibrahim, T.H., Burk, T.R., Etzler, F.M., Neuman, R.D., 2000. Direct adhesion measurements of pharmaceutical particles to gelatin capsule surfaces. *J. Adhes. Sci. Technol.* 14, 1225–1242.
- Israelachvili, J.N., 2002. *Intermolecular and Surface Forces*. Academic Press.
- Kim, S.H., Opdahl, A., Marmo, C., Somorjai, G.A., 2002. AFM and SFG studies of pHEMA-based hydrogel contact lens surfaces in saline solution: adhesion, friction, and the presence of non-crosslinked polymer chains at the surface. *Biomaterials* 23, 1657–1666.
- Lam, K.K., Newton, J.M., 1991. Investigation of applied compression on the adhesion of powders to a substrate surface. *Powder Technol.* 65, 167–175.
- Larson, I., Drammond, C.J., Chan, D.Y.C., Grieser, F., 1993. Direct force measurements between TiO<sub>2</sub> surfaces. *J. Am. Chem. Soc.* 115, 1185–1189.
- Lee, J., 2004. Intrinsic adhesion force of lubricants to steel surface. *J. Pharm. Sci.* 93, 2310–2318.
- Lee, J., 2005. Intrinsic adhesion properties of polyvinylpyrrolidone to pharmaceutical materials: humidity effect. *Macromol. Biosci.* 5, 1085–1093.
- Li, Y.Q., Tao, N.J., Pan, J., Garcia, A.A., Lindsay, S.M., 1993. Direct measurement of interaction forces between colloidal particles using the scanning force microscope. *Langmuir* 9, 637–641.
- Louey, M.D., Mulvaney, P., Stewart, P.J., 2001. Characterisation of adhesional properties of lactose carriers using atomic force microscopy. *J. Pharm. Biomed. Anal.* 25, 559–567.
- Mate, C.M., McClelland, G.M., Erlandsson, R., Chiang, S., 1987. Atomic-scale friction of a tungsten tip on a graphite surface. *Phys. Rev. Lett.* 59, 1942.
- Michrafy, A., Dodds, J.A., Kadiri, M.S., 2004. Wall friction in the compaction of pharmaceutical powders: measurement and effect on the density distribution. *Powder Technol.* 148, 53–55.
- Noy, A., Frisbie, C.D., Rozsnyal, L.F., Wrighton, M.S., Lieber, C.M., 1995. Chemical force microscopy: exploiting chemically-modified tips to quantify adhesion, friction, and functional group distributions in molecular assemblies. *J. Am. Chem. Soc.* 117, 7943–7951.
- Podczec, F., 1998a. Evaluation of the adhesion properties of salbutamol sulphate to inhaler materials. *Pharm. Res.* 15, 806–808.
- Podczec, F., 1998b. Adhesion forces in interactive powder mixtures of a micronized drug and carrier particles of various particle size distributions. *J. Adhes. Sci. Technol.* 12, 1323.
- Podczec, F., 1999. Investigations into the reduction of powder adhesion to stainless steel surfaces by surface modification to aid capsule filling. *Int. J. Pharm.* 178, 93–100.
- Podczec, F., Newton, J.M., James, M.B., 1995. Adhesion and friction between powders and polymer or aluminium surfaces determined by a centrifuge technique. *Powder Technol.* 83, 201–209.
- Sader, J.E., Larson, I., Mulvaney, P., White, L.R., 1995. Method for the calibration of atomic force microscope cantilevers. *Rev. Sci. Instrum.* 66, 3789–3798.
- Simons, S.J.R., Pepin, X., Rossetti, D., 2003. Predicting granule behavior through micro-mechanistic investigations. *Int. J. Miner. Process* 72, 463–475.
- Sindel, U., Zimmermann, I., 2001. Measurement of interaction forces between individual powder particles using atomic force microscope. *Powder Technol.* 117, 247–254.
- Tortonese, M., Kirk, M., 1997. Characterization of application specific probes for SPMs. *Micromachining and Imaging in Proceedings of SPIE—the International Society for Optical Engineering* 3009, 53–60.
- Tsukruk, V.V., Bliznyuk, V.N., 1998. Adhesive and friction forces between chemically modified silicone and silicone nitride surfaces. *Langmuir* 14, 446–455.
- Villarrubia, J.S., 1994. Morphological estimation of tip geometry for scanned probe microscopy. *Surf. Sci.* 321, 287–300.
- Xiao, X., Qian, L., 2000. Investigation of humidity-dependent capillary force. *Langmuir* 16, 8153–8158.
- Yoshizawa, H., Chen, Y.-L., Israelachvili, J., 1993. Fundamental mechanisms of interfacial friction. 1. Relation between adhesion and friction. *J. Phys. Chem.* 97, 4128.
- Yoshizawa, H., Israelachvili, J., 1994. Relation between adhesion and friction forces across thin films. *Thin Solid Films* 246, 71–76.